JACS
JOURNAL OF THE AMERICAN CHEMICAL SOCIETY
Communication
pubs.acs.org/JACS

Capture of Reactive Monophosphine-Ligated Palladium(0) Intermediates by Mass Spectrometry

Qiuling Zheng,[†] Yong Liu,[*,‡] Qinghao Chen,[*,‡] Meihong Hu,[†] Roy Helmy,[‡] Edward C. Sherer,[‡] Christopher J. Welch,[‡] and Hao Chen[*,†]

[†]Center for Intelligent Chemical Instrumentation, Department of Chemistry and Biochemistry, Edison Biotechnology Institute, Ohio University, Athens, Ohio 45701, United States

[‡]Department of Process and Analytical Chemistry and Department of Structural Chemistry, Merck Research Laboratories, Merck & Co., Inc., Rahway, New Jersey 07065, United States

Supporting Information

ABSTRACT: A long-sought-after reactive monophosphine-ligated palladium(0) intermediate, Pd^0L (L = phosphine ligand), was detected for the first time from the activation of the Buchwald precatalyst with base. The detection was enabled using desorption electrospray ionization mass spectrometry (DESI-MS) in combination with online reaction monitoring. The subsequent oxidative addition of Pd^0L with aryl halide and C−N coupling with amine via reductive elimination was also probed using DESI-MS.

Palladium-mediated cross-coupling reactions to form C−C, C−N, C−O, and C−S bonds (e.g., Buchwald−Hartwig aminations) are among the most powerful organometallic transformations employed in organic synthesis.[1−4] The catalytic reaction cycle typically involves three steps: (i) oxidative addition of Pd^0 with aryl halide, (ii) formation of palladium(II) complex through transmetalation, and (iii) regeneration of the active Pd^0 catalyst through reductive elimination. Evidence has been provided that the efficient formation of Pd^0, the presumed active catalyst, is the key to ensure the success of subsequent coupling reactions.[5−7] Commercially available Pd^0 species such as $Pd(PPh_3)_4$ and $Pd(dba)_3$ have many drawbacks which are well-documented in the literature.[8−11] In recent years, development and use of air-stable, readily activated palladium precatalysts has been the focus.[4,12−16] 2-Aminobiphenyl palladacycles developed by Buchwald's group are one of most important precatalysts.[11,17−21] The 2-aminobiphenyl palladacycles are activated by addition of base to undergo reductive elimination to form kinetically active Pd^0L. While dienes have been shown to be effective ancillary ligands to stabilize Pd^0L,[22] Pd^0L generated in situ in the absence of other stabilizing ligands has not been directly detected yet due to their high reactivity, air sensitivity, and ease of conversion to Pd(Ar)X(L) in the presence of ArX.[22−28] Widely used reaction monitoring techniques such as UV or IR spectroscopy are not specific, and very limited studies have been done by NMR spectroscopy.[29] The use of electrochemistry and cyclic voltammetry to study these short-lived intermediates offers some promise but does not provide the key structural information that is needed for detailed studies of reaction intermediates and mechanisms.

Mass spectrometry (MS) is a powerful technique for capturing and characterizing short-lived reaction intermediates since the advent of soft ionization methods such as electrospray ionization (ESI)[30−38] and desorption electrospray ionization (DESI).[39−42] ESI is a gentle ionization process which transfers products directly from liquid to the gas phase, and MS (and MS/MS) provides molecular weight and structural information. However, the solution composition can limit detection as ionization-favorable solvents or additives can obscure the observation of short-lived reactive intermediates. In this experiment, liquid sample DESI was used, as it is capable of ionizing the solution sample from native environments[43,44] and could be beneficial for short-lived intermediate characterization.

Herein, we present the direct capture of monophosphine-ligated Pd^0 intermediates generated from deprotonation of Buchwald precatalysts using online liquid sample DESI-MS. Scheme S1 (Supporting Information) shows the experimental setup configuration where a piece of fused silica capillary serves as a microreactor (20 cm in length, 100 μm i.d.), in which two reactant solutions (e.g., the Buchwald precatalyst and base) are mixed and introduced via a mixing Tee. With the injection flow rate set to 10 μL/min for each reactant, the reaction time was 9 s. Due to the air sensitivity of the reaction, all sample solvents and solutions were rigorously degassed with argon prior to mixing. The reaction solution exiting the capillary was continuously sampled using an impinging spray of charged microdroplets coming from the DESI source (DESI spray solvent: H_2O/MeOH (v/v 50:50) containing 1% formic acid, voltage = +5 kV, N_2 nebulization gas at 170 psi). Collision-induced dissociation (CID) was carried out for ion structural analysis. In this study, generation of the catalytically active Pd^0 species was initiated with online mixing of the Buchwald precatalyst palladium G3-(4-(*N*,*N*-dimethylamino)phenyl)di-*tert*-butylphosphine (G3, structure shown in Scheme 1, eq 1)[45] with sodium *tert*-butoxide (NaO^tBu).

Upon mixing G3 in THF (introduced through line A, Scheme S1) with THF (introduced through line B), a major ion corresponding to the cation of G3 at m/z 539 appeared in the acquired DESI-MS spectrum (Figure 1a). Figure 1b shows that once NaO^tBu in MeOH was introduced through line B and

Received: August 22, 2015
Published: October 26, 2015

DOI: 10.1021/jacs.5b08905
J. Am. Chem. Soc. 2015, 137, 14035−14038

Scheme 1

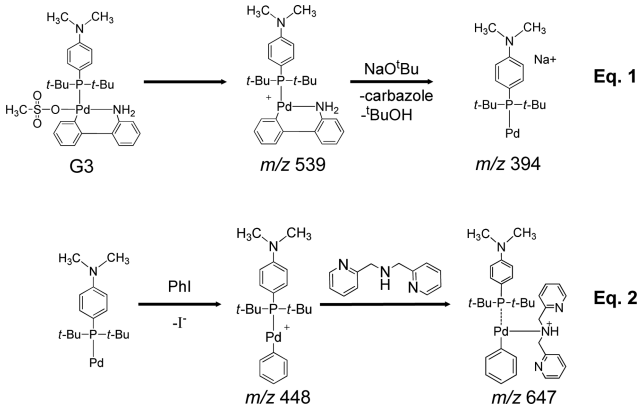

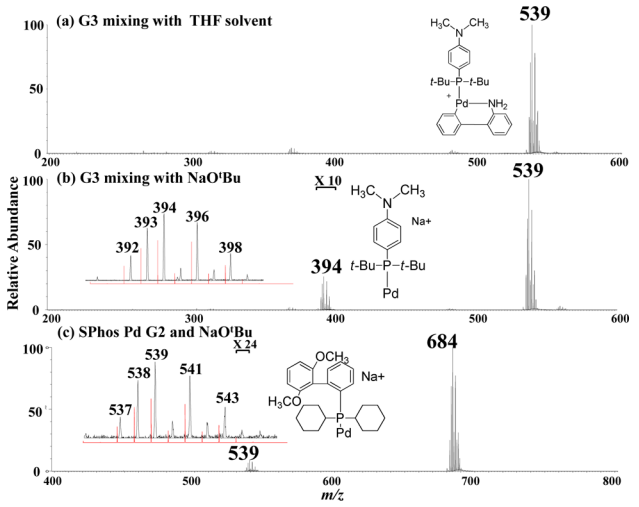

Figure 1. DESI-MS spectra of (a) G3 online mixed with solvent THF; (b) G3 online mixed with NaO^{t}Bu; and (c) SPhos Pd G2 online mixed with NaO^{t}Bu. Inset in (b) shows the zoomed-in spectrum of $[Pd^0L + Na]^+$ (m/z 394) generated from G3 (in black) and its theoretical isotopic peak distribution (in red). Inset in (c) shows the zoomed-in spectrum of $[Pd^0L + Na]^+$ (m/z 539) generated from SPhos Pd G2 (in black) and its theoretical isotopic peak distribution (in red).

online mixed with G3, the sodium-adducted Pd^0L species at m/z 394 was formed and immediately captured by MS (eq 1). It is reasonable that sodiated Pd^0L rather than the protonated Pd^0L was detected because the reaction mixture has excess NaO^{t}Bu. The inset in Figure 1b clearly shows the zoomed-in spectrum of $[Pd^0L + Na]^+$ at m/z 394 (in black), which exactly matches its theoretical isotopic peak distribution (in red).

Furthermore, the CID MS/MS of m/z 394 (Figure S1a, Supporting Information) gives rise to a fragment ion m/z 338 by loss of isobutene, consistent with the assigned ion structure. To confirm that the observed $[Pd^0L + Na]^+$ was not from background interference, a control experiment was performed by online mixing G3 with sodium tetrafluoroborate ($NaBF_4$) instead of NaO^{t}Bu. No formation of m/z 394 (Figure S2a) was observed, which supported the requirement of base for triggering the formation of the Pd^0L species. In this case, Na^+ serves as a charge carrier to facilitate detection of the Pd^0L species by MS. Similarly, replacement of NaO^{t}Bu with KO^{t}Bu led to observation of the potassium-adducted Pd^0L detected at m/z 410 (Figure S2b), as expected. Furthermore, the reaction of another Buchwald precatalyst, chloro(2-dicyclohexylphosphino-2′,6′-dimethoxy-1,1′-biphenyl)[2-(2′-amino-1,1′-biphenyl)]-palladium(II) (SPhos Pd G2),[5] with NaO^{t}Bu was examined. Besides the dominant cation of SPhos Pd G2 appearing at m/z 684, the sodium-adducted Pd^0L species at m/z 539 was also observed (Figure 1c), and its structure was confirmed by CID MS/MS (Figure S1b). These MS results provide the first direct evidence for the formation of the Pd^0L species. Interestingly, attempts at detecting Pd^0L species by ESI-MS using the same reaction conditions failed, probably due to oxidation of the Pd^0L intermediate from inherent electrochemical oxidation during ESI ionization (Figure S3). In contrast, no high voltage needs to be applied to the reaction solution sample in DESI-MS.

Calculation of the sodiated Pd^0L species from G3 was also carried out to better understand the ion structure. The global minimum (Figure 2) is characterized by a sodium cation

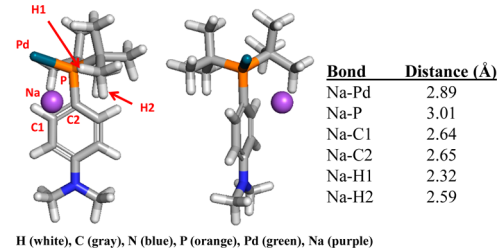

Bond	Distance (Å)
Na-Pd	2.89
Na-P	3.01
Na-C1	2.64
Na-C2	2.65
Na-H1	2.32
Na-H2	2.59

Figure 2. Global energy minimum structure of $[Pd^0L + Na]^+$ (m/z 394) from G3 as obtained using B3LYP-D2 (5 other minima are depicted in Figure S7). The global minimum is at least 2.4 kcal/mol lower in energy compared to that of all other complex geometries (ΔG).

coordinated to Pd^0L through three different types of interactions: cation−π to the phenyl ring, Pd coordination, and van der Waals contact to one methyl of the *tert*-butyl group. While cation−π[46,47] interactions might be expected to dominate the coordination configuration, the sodium interaction is split across the modes listed above. The multidentate nature of the sodium coordination has been observed in calculated geometries for Na^+/K^+ complexes to aromatic amino acids.[48]

Not surprisingly, DESI-MS studies revealed that the Pd^0L species is unstable and short-lived. Slowing down the flow rates for incoming reagents corresponds to increasing reaction time within the capillary microreactor, which leads to the formation of a stable sodium-adducted Pd^0L_2 complex at m/z 659 (Figure S4). When the flow rate was 10 μL/min (i.e., the reaction time of 9 s), there was no m/z 659 detected. Upon decreasing the flow rate to 5 and 1 μL/min (i.e., increase the reaction time to 18 and 90 s, respectively), Pd^0L began to convert into Pd^0L_2 and was detected as $[Pd^0L_2 + Na]^+$ by observing the significant intensity increment of m/z 659 (Figure S4).

According to the established mechanistic understanding for Pd-catalyzed C−N coupling,[25] the active Pd intermediate is expected to undergo oxidative addition with aryl halide, ArX,[49] followed by addition of an amine substrate and deprotonation to generate the Pd(II)−amine complex, which further undergoes reductive elimination to afford the final C−N coupling product (Scheme 2). With the ability to detect the catalytically reactive Pd^0L species using the DESI-MS approach, we set out to investigate the ability to detect other species within the reaction cycle. Premixing G3 with iodobenzene (PhI), and further mixing with NaO^{t}Bu, allowed the in situ generated Pd^0L species to undergo oxidative addition with PhI (eq 2, Scheme 1) to produce $[LPdPh]^+$, which was successfully observed at m/z 448 (Figure 3a). The inset in Figure 3a shows that the actual isotopic peak

DOI: 10.1021/jacs.5b08905
J. Am. Chem. Soc. 2015, 137, 14035−14038

Scheme 2. Proposed General Mechanism for the Pd-Catalyzed C−N Coupling Reaction

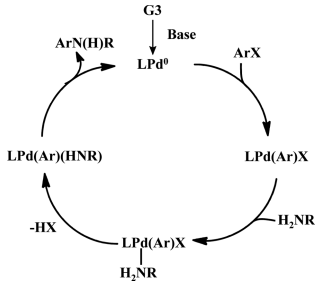

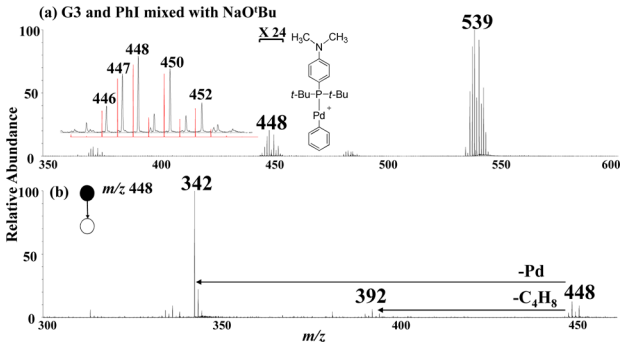

Figure 3. (a) DESI-MS spectrum of G3 and PhI in THF online mixed with NaO^{t}Bu in MeOH, and (b) CID MS/MS spectrum of m/z 448. Inset in (a) shows the zoomed-in spectrum of the oxidative addition product ion $[LPdPh]^+$ at m/z 448 (in black) and its theoretical isotopic peak distribution (in red).

distribution for $[LPdPh]^+$ (in black) is identical to that of the theoretical prediction (in red). CID MS/MS confirms the assigned ion structure by yielding fragment ions of m/z 392 and 342 via losses of isobutene and Pd (Figure 3b). The observation of the ion $[LPdPh]^+$ resulting from the oxidative addition product is probably due to facile loss of the iodide anion.

To investigate the subsequent C−N coupling reaction, 2,2′-dipicolylamine containing a secondary amine functional group was chosen as an amine substrate and premixed with NaO^{t}Bu in line B, while G3 and PhI were kept in line A. Besides the observation of Pd^0L (m/z 394) and $[LPdPh]^+$ (m/z 448), generation of a new set of peaks at m/z 647 indicated the successful formation and detection of the Pd^{II}−amine complex, $[LPd^{II}Ph(HNR_2)]^+$ (Figure 4a). Upon CID (Figure 4b), a major fragment ion at m/z 382 was generated by the loss of phosphine ligand L rather than the loss of the bound amine, which suggested the quite strong binding between amine and Pd. In addition, the observation of m/z 276, corresponding to the protonated *N*,*N*-bis(pyridin-2-ylmethyl)aniline, indicates the generation of the C−N coupling final product (structure shown in the inset of Figure 4a). The observation of the protonated species rather than sodiated species for the final product and the Pd^{II}−amine complex is probably due to their high proton affinities. Therefore, via the final reductive elimination, the catalytic cycle is completed, with both products and intermediates being observed by the DESI-MS technique. Besides 2,2′-dipicolylamine, three additional amine substrates including pyrrolidine, *N*-methylpropylamine, and piperidine were examined, and similar results were obtained (Table S1).

In addition to the C−N coupling reaction, the C−C coupling reaction was also explored by online mixing precatalyst, pyridine halide, and phenyl boronic acid in the presence of base. Likewise,

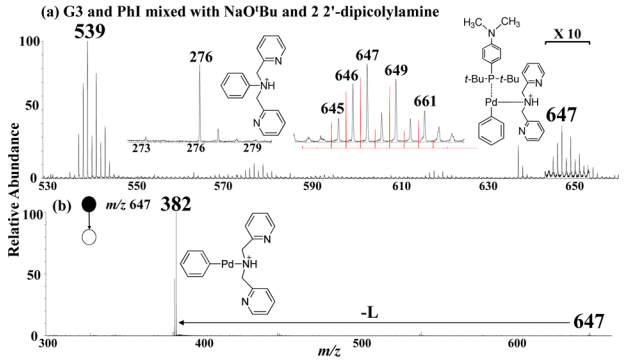

Figure 4. (a) DESI-MS spectrum of G3 and PhI in THF online mixed with NaO^{t}Bu and 2,2′-dipicolylamine in MeOH, and (b) CID MS/MS spectrum of the Pd^{II}−amine complex ion at m/z 647. Insets in (a) show the zoomed-in spectra of the protonated *N*,*N*-bis(pyridin-2-ylmethyl)-aniline (m/z 276) and the protonated Pd(II)−amine complex at m/z 647 (in black) along with its theoretical isotopic peak distribution (in red).

the Pd^{II}−phenyl boronic acid intermediates and final products were also successfully detected by DESI-MS (see Table S2, Figures S5 and S6, and discussion in Supporting Information). This study, for the first time, presents the detection of the reactive monophosphine-ligated Pd^0L intermediate from reaction solution by MS, which has been long regarded as the true reaction intermediate in various Pd-catalyzed coupling reactions but has not yet been directly observed. Using the C−N and C−C couplings as a demonstration, we detected other important reaction intermediates and the final products resulting from the initial Pd^0L intermediate, providing insight into the reaction mechanisms. The in situ ionization capability and solvent tolerance of DESI facilitate the observation of otherwise short-lived and difficult-to-study reactive intermediates, requiring only a minimal amount of sample and utilizing fairly straightforward MS instrumentation. These advantages suggest the further potential of DESI-MS in the study of reactive intermediates and the elucidation of reaction mechanisms.

■ ASSOCIATED CONTENT

Supporting Information

The Supporting Information is available free of charge on the ACS Publications website at DOI: 10.1021/jacs.5b08905.

Computational calculation method and additional MS and MS/MS data (PDF)

■ AUTHOR INFORMATION

Corresponding Authors

*yong_liu2@merck.com
*qinghao_chen@merck.com
*chenh2@ohio.edu

Notes

The authors declare no competing financial interest.

■ ACKNOWLEDGMENTS

This work was supported by generous funding from the Merck Research Laboratories New Technologies Review & Licensing Committee (NT-RLC) and by NSF Career Award (CHE-1149367), NSF IDBR (CHE-1455554), and NNSFC (21328502). We also thank Dr. Kevin Campos and Dr. Zhijian Liu for helpful discussion and suggestions.

DOI: 10.1021/jacs.5b08905
J. Am. Chem. Soc. 2015, 137, 14035−14038

REFERENCES

(1) Christmann, U.; Vilar, R. *Angew. Chem., Int. Ed.* **2005**, *44*, 366−374.
(2) Martin, R.; Buchwald, S. L. *Acc. Chem. Res.* **2008**, *41*, 1461−1473.
(3) Hartwig, J. F. *Nature* **2008**, *455*, 314−322.
(4) Organ, M. G.; Abdel-Hadi, M.; Avola, S.; Dubovyk, I.; Hadei, N.; Kantchev, E. A. B.; O'Brien, C. J.; Sayah, M.; Valente, C. *Chem. - Eur. J.* **2008**, *14*, 2443−2452.
(5) Surry, D. S.; Buchwald, S. L. *Angew. Chem., Int. Ed.* **2008**, *47*, 6338−6361.
(6) Garcia-Melchor, M.; Braga, A. A. C.; Lledos, A.; Ujaque, G.; Maseras, F. *Acc. Chem. Res.* **2013**, *46*, 2626−2634.
(7) Bonney, K. J.; Schoenebeck, F. *Chem. Soc. Rev.* **2014**, *43*, 6609−6638.
(8) Amatore, C.; Broeker, G.; Jutand, A.; Khalil, F. *J. Am. Chem. Soc.* **1997**, *119*, 5176−5185.
(9) Urgaonkar, S.; Verkade, J. G. *J. Org. Chem.* **2004**, *69*, 9135−9142.
(10) Zalesskiy, S. S.; Ananikov, V. P. *Organometallics* **2012**, *31*, 2302−2309.
(11) Bruneau, A.; Roche, M.; Alami, M.; Messaoudi, S. *ACS Catal.* **2015**, *5*, 1386−1396.
(12) Beletskaya, I. P.; Cheprakov, A. V. *J. Organomet. Chem.* **2004**, *689*, 4055−4082.
(13) Li, H.; Johansson Seechurn, C. C. C.; Colacot, T. J. *ACS Catal.* **2012**, *2*, 1147−1164.
(14) Colacot, T. J., Ed. *New Trends in Cross-Coupling: Theory and Applications*; RSC: London, 2015; 864 pp.
(15) Guram, A. S.; Wang, X.; Bunel, E. E.; Faul, M. M.; Larsen, R. D.; Martinelli, M. J. *J. Org. Chem.* **2007**, *72*, 5104−5112.
(16) Guram, A. S.; King, A. O.; Allen, J. G.; Wang, X.; Schenkel, L. B.; Chan, J.; Bunel, E. E.; Faul, M. M.; Larsen, R. D.; Martinelli, M. J.; Reider, P. J. *Org. Lett.* **2006**, *8*, 1787−1789.
(17) Bruno, N. C.; Tudge, M. T.; Buchwald, S. L. *Chem. Sci.* **2013**, *4*, 916−920.
(18) Biscoe, M. R.; Fors, B. P.; Buchwald, S. L. *J. Am. Chem. Soc.* **2008**, *130*, 6686−6687.
(19) Kinzel, T.; Zhang, Y.; Buchwald, S. L. *J. Am. Chem. Soc.* **2010**, *132*, 14073−14075.
(20) Bruno, N. C.; Buchwald, S. L. *Org. Lett.* **2013**, *15*, 2876−2879.
(21) Bruno, N. C.; Niljianskul, N.; Buchwald, S. L. *J. Org. Chem.* **2014**, *79*, 4161−4166.
(22) Andreu, M. G.; Zapf, A.; Beller, M. *Chem. Commun.* **2000**, 2475−2476.
(23) Vidossich, P.; Ujaque, G.; Lledos, A. *Chem. Commun.* **2014**, *50*, 661−663.
(24) Christmann, U.; Vilar, R. *Angew. Chem., Int. Ed.* **2005**, *44*, 366−374.
(25) Barrios-Landeros, F.; Carrow, B. P.; Hartwig, J. F. *J. Am. Chem. Soc.* **2009**, *131*, 8141−8154.
(26) Braga, A. A. C.; Ujaque, G.; Maseras, F. *Organometallics* **2006**, *25*, 3647−3658.
(27) Schoenebeck, F.; Houk, K. N. *J. Am. Chem. Soc.* **2010**, *132*, 2496−2497.
(28) McMullin, C. L.; Fey, N.; Harvey, J. N. *Dalton Trans.* **2014**, *43*, 13545−13556.
(29) Casado, A. L.; Espinet, P.; Gallego, A. M.; Martinez-Ilarduya, J. M. *Chem. Commun.* **2001**, 339−340.
(30) Sabino, A. A.; Machado, A. H. L.; Correia, C. R. D.; Eberlin, M. N. *Angew. Chem., Int. Ed.* **2004**, *43*, 2514−2518.
(31) Zavras, A.; Khairallah, G. N.; Connell, T. U.; White, J. M.; Edwards, A. J.; Donnelly, P. S.; O'Hair, R. A. J. *Angew. Chem., Int. Ed.* **2013**, *52*, 8391−8394.
(32) Meyer, M. M.; Khairallah, G. N.; Kass, S. R.; O'Hair, R. A. J. *Angew. Chem., Int. Ed.* **2009**, *48*, 2934−2936.
(33) Bao, H.; Zhou, J.; Wang, Z.; Guo, Y.; You, T.; Ding, K. *J. Am. Chem. Soc.* **2008**, *130*, 10116−10127.
(34) Wilson, S. R.; Perez, J.; Pasternak, A. *J. Am. Chem. Soc.* **1993**, *115*, 1994−1997.
(35) Feichtinger, D.; Plattner, D. A.; Chen, P. *J. Am. Chem. Soc.* **1998**, *120*, 7125−7126.
(36) Julian, R. R.; May, J. A.; Stoltz, B. M.; Beauchamp, J. L. *J. Am. Chem. Soc.* **2003**, *125*, 4478−4486.
(37) Feichtinger, D.; Plattner, D. A. *Angew. Chem., Int. Ed. Engl.* **1997**, *36*, 1718−1719.
(38) Yunker, L. P. E.; Stoddard, R. L.; McIndoe, J. S. *J. Mass Spectrom.* **2014**, *49*, 1−8.
(39) Takáts, Z.; Wiseman, J. M.; Gologan, B.; Cooks, R. G. *Science* **2004**, *306*, 471−473.
(40) Brown, T. A.; Chen, H.; Zare, R. N. *J. Am. Chem. Soc.* **2015**, *137*, 7274−7277.
(41) Perry, R. H.; Splendore, M.; Chien, A.; Davis, N. K.; Zare, R. N. *Angew. Chem., Int. Ed.* **2011**, *50*, 250−254.
(42) Perry, R. H.; Brownell, K. R.; Chingin, K.; Cahill, T. J., III; Waymouth, R. M.; Zare, R. N. *Proc. Natl. Acad. Sci. U. S. A.* **2012**, *109*, 2246−2250.
(43) Miao, Z.; Wu, S.; Chen, H. *J. Am. Soc. Mass Spectrom.* **2010**, *21*, 1730−1736.
(44) Ferguson, C. N.; Benchaar, S. A.; Miao, Z.; Loo, J. A.; Chen, H. *Anal. Chem.* **2011**, *83*, 6468−6473.
(45) Muci, A.; Buchwald, S. In *Cross-Coupling Reactions*; Miyaura, N., Ed.; Springer: Berlin, 2002; pp 131−209.
(46) Dougherty, D. A. *Science* **1996**, *271*, 163−168.
(47) Ma, J. C.; Dougherty, D. A. *Chem. Rev.* **1997**, *97*, 1303−1324.
(48) Ruan, C.; Rodgers, M. T. *J. Am. Chem. Soc.* **2004**, *126*, 14600−14610.
(49) Vikse, K.; Naka, T.; McIndoe, J. S.; Besora, M.; Maseras, F. *ChemCatChem* **2013**, *5*, 3604−3609.

DOI: 10.1021/jacs.5b08905
J. Am. Chem. Soc. 2015, 137, 14035−14038